Adipogenic Mesenchymal Stem Cells and Hyaluronic Acid as a Cellular Compound for Bone Tissue Engineering

Daniel Goncalves Boeckel, DDS, PhD,* Patrícia Sesterheim, DMSc, PhD,†
Thiago Rodrigues Peres, DDS,† Adolpho Herbert Augustin, DDS,‡
Krista Minéia Wartchow, DMSc,§ Denise Cantarelli Machado, DMSc, PhD,‖
Guilherme Genehr Fritscher, DDS, PhD,¶ and Eduardo Rolim Teixeira, DDS, PhD*

Abstract: This study investigates the applicability of adipose mesenchymal stem cells (mADSCs) and hyaluronic acid (HA) as a cellular compound for bone tissue engineering. A critical bone defect was created on each femur of 25 rats in vivo, receiving the following 5 graft treatments: I—Control-defect; II—HA; III—mADSCs; IV—mADSCs+HA; and V—previously osteoinduced mADSCs+HA. Evaluation using microcomputed tomography, histomorphometry, and RT-PCR analysis was performed 23 days after implantation. Microcomputed tomography analysis indicated higher means of bone contact surface (BCS) and bone surface density (BSD) for the mADSCs+HA group compared with Control and the HA groups ($P < 0.05$). Histomorphometric findings showed higher means of bone regeneration in the mADSCs+HA compared with HA and Control groups ($P < 0.05$). The RT-PCR ratios showed no difference in type 1 collagen (Col1A) gene expression or osteopontin (OP) gene expression, whereas for the osteonectin gene (ON) higher means were found in the HA and mADSCs osteoin+HA groups ($P < 0.05$). These results suggest that a combination of HA and mADSCs without prior osteoinduction might be applicable for bone tissue regeneration.

Key Words: Adipose mesenchymal stem cells, bone regeneration, hyaluronic acid, tissue engineering

(J Craniofac Surg 2019;30: 777–783)

Several types of biomaterials are nowadays available for bone grafting; however, autogenous grafts are still believed to be the "gold standard" when considering bone reconstruction, mainly due to an absence of immune response during the remodeling process, unlike allogeneic and xenogeneic grafts, which may carry a greater risk of pathogen transmission, immunologic reactions, and cross-linked infections.[1] Still, the use of autogenous bone grafts presents important limitations, mainly related to the amount of tissue available for grafting, the risk of partial necrosis-associated insufficient revascularization, and also higher surgical morbidity.[1,2]

As a promising alternative to conventional autografts, techniques involving tissue-engineered ex vivo cell manipulation, combined or not with growth factors and specific matrices, have been widely reported in the literature in recent decades.[3–9] The potential use of tissue engineering as an applicable option in Orthopedics and Dentistry has been emphasized due to promising early results.[7] In Dentistry, it may be applied as a reparative technique to a variety of tissues such as bone, cartilage, skin, oral mucosa, dentine, dental pulp, and salivary glands.[10]

Mesenchymal stem cells (MSCs) have been used in tissue engineering mainly because of their pluripotent nature, availability, and potential for differentiation, generating expressive results in terms of tissue regeneration.[11] Mesenchymal stem cells collected from bone marrow were the first cells reported to display fibroblast-like cell behavior and to adhere to plastic culture flasks in vitro.[12] Mesenchymal stem cells also secrete a variety of cytokines and growth factors presenting reported paracrine and autocrine activities, which are fundamental properties to the observed therapeutic effects.[13] These secreted cytokines present antiapoptotic and pro-angiogenic actions, as well as potential endogenous reparative effects.[14,15] Moreover, these trophic factors regulate a series of osteogenic and angiogenic events, cell migration, proliferation, and osteoblast differentiation.[16,17] Another very important characteristic of MSCs is their immunosuppressive action, associated with their ability to accumulate around regions of inflammation and cause a local change in the immune response profile, from proinflammatory to anti-inflammatory.[18]

Also, the presence of available scaffold for facilitating cell adhesion and proliferation has been said to be a key for tissue formation when considering tissue engineering.[10] In this regard, during the search for applicable biomaterials capable of improving graft response, hyaluronic acid (HA) has emerged as a promising alternative, being a major component of the extracellular matrix in the connective tissue.[18] It also participates in biological processes involving morphogenesis, wound healing, inflammation, and metastasis through cellular receptors.[19] Hyaluronic acid is composed of repeated disaccharide units containing glucuronic acid and N-acetylglucosamine.[20] It has an essential role in the structure and organization of the extracellular matrix, and its hydrating capacity may facilitate cell detachment, thus enabling cell migration.[21] However, the interaction of HA in the form of a hydrogel with adipose MSCs in vivo as a graft compound has not been thoroughly evaluated.[22]

Given the basic characteristics of MSCs and HA, their combination as a graft compound might lead to a promising alternative for bone bioengineering. The present study aimed at evaluating the

effect of multipotent adipose-derived stromal cells (mADSCs) combined with a low-molecular-weight (500–730 kDa) HA scaffold in the form of a hydrogel on an in vivo surgically-induced bone critical defect regeneration animal model.

METHODS

Animals

Five male Lewis rats were used as cell donors for the isolation of the mADSCs. Other 25 male rats of the same strain received a surgically-induced critical bone defect in both right and left femurs for the subsequent tests. Both the donor and recipient animals weighed approximately 300 to 315 g. The animals, which were specific pathogen-free, were housed under controlled photoperiod (day/night) and temperature (22°C). They were kept in cages (maximum 4 animals/cage), properly identified, fed Nuvilab CR-1 standard rodent feed (Nuvital, Curitiba, Paraná, Brazil) and given water ad libitum. This study was conducted after approval by the Ethics Committee for Animal Use of the Pontifical Catholic University of Rio Grande do Sul (PUCRS) (Protocol 52/201-CEUA).

Cell Culture and Osteogenic Differentiation

Following a previously described methodology, Meirelles and Nardi,[23] murine adipose-derived stem cells (mASCs) were isolated from the epididymal fat of Lewis rats euthanized by CO_2 inhalation.

The protocol was based on tissue dissociation for the preparation of cell suspensions. A pubic incision was made, and an epididymal fat fragment ($5 mm^3$) was removed, washed in Hank solution, lightly perforated, and transferred to a 15 mL Falcon tube containing 3 mL of a sterile solution of 1.5 g/mL collagenase type 1 (Gibco) dissolved in DMEM plus 3.7 g/L sodium bicarbonate (Sigma) and 2.5 g/L serum-free (4-(2-hydroxyethyl)-1-piperazineethanesulfonic acid) (HEPES, Sigma). The sample was incubated in a water bath at 37°C for 20 to 25 min. After the digestion period, the fragments were mechanically dissociated and homogenized with the aid of a Pasteur pipette and 10 mL of culture medium (CM) was added; the CM consisted of Dulbecco's Modified Eagle Medium/low glucose (DMEM, Gibco BRL, Gaithersburg, MD), 3.7 g/L sodium bicarbonate (this reagent and all others were obtained from Sigma, St Louis, MO, unless otherwise indicated), 2.5 g/L HEPES, 10% fetal bovine serum (FBS) (Cultilab, SP, Brazil), and 1% penicillin/streptomycin (Gibco). After centrifuging for 10 minutes at 1500 rpm, the supernatant was discarded, and the pellet was resuspended in 4 mL of CM. The supernatant was decanted and transferred to 6-well plates (TPP, Trasadingen, Switzerland), in which the cultures were maintained until they reached a minimum confluence of 80% in a humidified incubator at 37°C under a 5% CO_2 atmosphere. The replating rate (P-passage) was determined based on the culture kinetics.

The cells were maintained in culture medium (CM) composed of Dulbecco's Modified Eagle's Medium/low glucose (DMEM, Gibco BRL, Gaithersburg, MD) with 3.7 g/L sodium bicarbonate (Sigma,

Saint Louis, MO), 2.5 g/L HEPES, 10% fetal bovine serum (FBS) (Cultilab, São Paulo, SP, Brazil) and 1% penicillin/streptomycin (Gibco). After the functional criteria compatible with true MSCs, such as immunophenotypic profile, adherence to plastic and ability to form adipocytes and osteoblasts were confirmed, the cells were divided into 2 groups, being one comprised of undifferentiated mADSCs used at the 4th passage (P4) and the other subjected to an osteogenic differentiation protocol. This protocol consisted of growth for 4 weeks in CM supplemented with 10^{-5}M dexamethasone, 5 μg/mL ascorbic acid 2-phosphate and 10 mM β-glycerophosphate. Osteoblasts were identified by staining the calcium deposition with Alizarin Red S stain at pH 4.2. Once differentiated, the cells secrete a calcium-rich extracellular matrix, which was revealed using Alizarin Red S dye.

Surgical Procedures and Treatments

To analyze the integration of undifferentiated mADSCs, mADSCs transdifferentiated into osteoblasts and the in vivo osteoconductive role of HA scaffold–hydrogel (Hyaloss, META, Reggio Emilia, Italy) in bone defects, 25 Lewis rats were used. Following anesthesia with 10% ketamine hydrochloride combined with 2% xylazine chloride (100 mg/kg intraperitoneally), antisepsis was performed topically with 1% polyvinylpyrrolidone at the surgical site. A longitudinal incision of approximately 2 cm was made parallel and anterior to the axis of both femurs. The area anterior to each femur was exposed by gentle separation of the muscle planes and periosteum. Surgical bone defects were created by low-speed drilling with a round bur (K Driller SMART, Carapicuíba, SP, Brazil) under profuse irrigation with 0.9% saline. Each animal was subjected to 2 monocortical critical defects 2 mm wide and 2.5 mm deep, one on the right femur and one on the left femur, classified according to the received treatment (Table 1). The mixture of the hyaloss gel with the cells occurred at the moment of grafting, placing the gel in the defect bed and later the cells on the gel. Tissues were sutured with 4-0 polyglactin, and a benzoin tincture was applied around the wound. After surgery, the animals received analgesia with Tramadol (12.5 mg/kgip) every 8 hours for 4 days.

Twenty-three days later, the animals were euthanized by anesthetic injection (100 mg/kg thiopental combined with 10 mg/mL of lidocaine). Five femurs in each group were first collected and stored in 10% formalin in labeled bottles. Then, they were submitted for specimen processing and later for micro-CT and histomorphometric analysis. Five other femurs from each experimental group, also properly identified, were stored in Eppendorf vials with RNALater (Sigma) for RT-PCR analysis. The time of 23 days was due to the size of the critical defect realized, that is, in that period the defect created does not suffer spontaneous repair.

Microcomputer Tomography (Micro-CT) Analysis

Tomographic images were acquired using a 70 Kv-f114 μA micro-CT scanner (Sky Scan 1173, Bruker, Billerica, MA) set to

TABLE 1. Treatments and Sample n for the Experimental Groups

Treatment/Group	n	mADSC (Undifferentia-ted Cells	mADSC osteoin (Osteoinduced Cells)	HA (Hyaluronic Acid)
I—Control (C)	10	—	—	—
II—HA	10	—	—	0.8 mg
III—mADSCs	10	1×10^7	—	—
IV—mADSCs+HA	10	1×10^7	—	0.8 mg
V—mADSCsosteoin+HA	10	—	1×10^7	0.8 mg

a resolution of 6 microns. The images were reconstructed and analyzed and newly formed bone tissue was quantified (CT Analyzer software version 1.14.4.1).

After images were acquired, a circular region of interest (ROI) was established and standardized for all analyzed defects. A 2 mm wide and 1 mm deep ROI was established, comprising the area from the edge of the defect to the medullar bone of the femur. After grayscale tuning, which ranged from 0 to 255 bytes, the gray patterns were selected manually to ensure the best tomographic data within the ROI, to differentiate the mineralized tissue from the soft tissue within the critical defect. Subsequent to 3D image reconstruction, the following morphometric parameters were obtained: bone contact surface, being the surface area of interconnected mineralized tissue (mm^2), and bone density surface, being the ratio of total mineralized tissue surface area by the total analyzed volume (BDS/TV; mm^2/mm^3).

Histomorphometric Analysis

Following removal of the right and left femurs, bone blocks containing the tested sites were cut and decalcified with 5% HNO_3. The blocks were dehydrated in a graded alcohol series, clarified with xylene and embedded in paraffin. Using a microtome, a total of three 3-μm-thick slices from each paraffin block were sectioned transversely to each femur's long axis at 300, 600, and 900 μm from the external cortical bone adjacent to the critical defect. After routine staining with hematoxylin-eosin (HE), microscopic analysis was performed at ×24 magnification using an optical stereo microscope (Zeiss stemi DV4, Gottingen, Germany) connected to a digital camera (SonyDSC P-92, Sony Inc, Tokyo, Japan). Image analysis was performed using the ImageJ software (v.1.49 for Windows, Media Cybernetics, Silver Spring, MD).

The serial cross-sections were evaluated by a single blinded examiner who quantified the area of new bone inside the defect using a pixel scale. The intraclass correlation coefficient was obtained to allow analysis of the data reproducibility on each measurement, and considered excellent when coefficient values were greater than 0.75. Two measurements of each sample were obtained for this calculation, and the measurements were performed by the same examiner with a 1-week interval between measurements, obtaining an intraclass correlation coefficient of 0.975.

Real-Time Reverse Transcriptase-Polymerase Chain Reaction Analysis (RT-PCR)

Real-time reverse transcriptase-polymerase chain reaction (RT-PCR) analysis was performed as previously described.[24,25] RNA extraction was performed using RNA SV-Total (Promega Life Sciences, Madison, WI) according to the manufacturer's instructions. The amount of total RNA was assessed using a Qubit 2.0 Fluorometer (Invitrogen, Carlsbad, CA). The synthesis of cDNA was performed using SuperScript VILO MasterMix (Life Technologies, Carlsbad, CA) according to the manufacturer's instructions. Each reaction used 20 ng of cDNA. Quantitative real-time RT-PCR was performed using SYBR Select Master Mix (Applied Biosystems, Foster City, CA) on a Step One Plus Real-Time PCR System thermal cycler (Applied Biosystems). The endogenous control gene was glyceraldehyde 3-phosphate dehydrogenase (GAPDH). The $2^{-\Delta\Delta ct}$ method was used for quantitative analysis of the data.

Statistical Analysis

The means of the micro-CT and histological measurements presented a normal distribution according to the Kolmogorov–Smirnov test. Analysis of variance (ANOVA) was performed for each measurement, and when a statistically significant difference

was observed, Tukey post-hoc test for multiple comparisons was used. The RT-PCR variable did not fit a normal distribution according to the Kolmogorov–Smirnov test; therefore, comparison between groups was performed using the Kruskal–Wallis nonparametric test. In all statistical tests, a significance level of 5% ($P < 0.05$) was adopted. Database creation and statistical analyses were performed using SPSS software version 17.0.

RESULTS

Osteogenic Transdifferentiation of Multipotent Adipose-Derived Stromal Cells

The mADSCs undergoing osteogenic differentiation maintained a fusiform appearance similar to that of noninduced cells and showed an increase in alkaline phosphatase activity and deposition of a calcium-rich extracellular matrix as evidenced by Alizarin Red S staining.

Microcomputed Tomography

The micro-CT results for bone contact surface (BCS) and bone density surface (BDS) are shown in Figure 1A and B, respectively. The BCS and BDS evaluation revealed that cell groups III (BCS mean: 96.68 $mm^2 \pm 24.02$; BDS mean: 15.46 $mm^2/mm^3/\pm 2.57$), IV (BCS: 105.11 $mm^2 \pm 15.76$; BDS 16.60 $mm^2/mm^3 \pm 2.89$) and V (BCS: 95.62 $mm^2 \pm 9.84$; BDS: 15.58 $mm^2/mm^3 \pm 1.53$) had higher BCS and BDS values than the cell-free groups I (BCS: 62.58 $mm^2 \pm 10.86$; BDS: 10.16 $mm^2/mm^3 \pm : 1.57$) and II (BCS: 61.94 $mm^2 \pm : 13.51$; BDS: 9.93 $mm^2/mm^3 \pm 2.64$) ($P < 0.05$). When the cell groups were compared to each other, group V had slightly lower performance than groups III and IV in regard to BCS, although these groups did not differ statistically across all parameters. Tomographic images of the bone surface, internal and ROI views of all treatments are shown in Figure 2.

Histomorphometry

Histomorphometric analysis using a specific software (ImageJ, US National Institutes of Health, Bethesda, MD) indicated greater bone regeneration area in groups III (mean: 2.26 $mm^2 \pm 0.54 mm^2$), IV (2.42 $mm^2 \pm 0.25 mm^2$) and V (2.32 $mm^2 \pm 0.32 mm^2$) with a statistically significant difference compared to groups I and II (Fig. 1C).
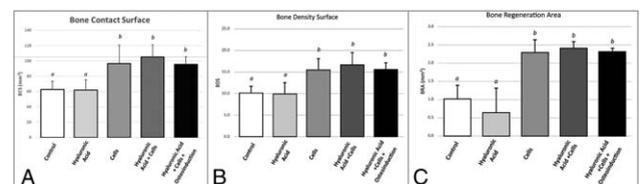

FIGURE 1. (A) Mean and standard deviation of bone contact surface (BCS) of the control group and treatment groups II, III, IV, and V. The mADSCs + HA group shows the highest mean BCS value, followed by the mADSCs group and the mADSCs osteoinduced + HA group; both of the latter groups differed significantly from the C and HA groups, which displayed the lowest mean values ($P < 0.05$). The mean values of the groups indicated by the same letters are not significantly different from each other. (B) Mean and standard deviation of bone density surface (BDS) of the control group and treatment groups II, III, IV, and V. The mADSCs + HA group displays the highest mean, followed by the mADSCs osteoinduced + HA and mADSCs groups; all 3 of these groups differ significantly from the C (I) and HA (II) groups, which had the lowest means ($P < 0.05$). Different letters indicate a statistical significance between the analyzed groups. (C) Mean and standard deviation of the bone regeneration area within the bone defect area after 23 days. The highest means were observed in the mADSCs + HA group, followed by the mADSCs osteoin + HA and mADSCs groups. The HA group had the lowest mean, followed by the C group. Different letters indicate a statistically significant difference ($P < 0.05$).
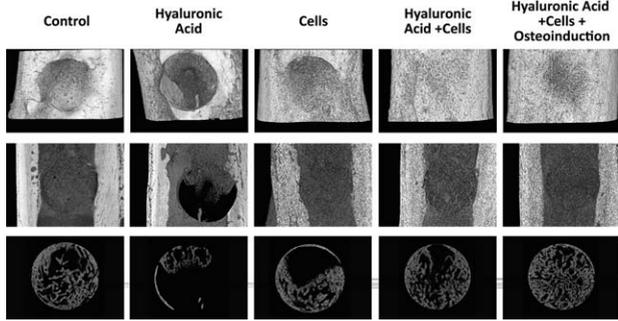
FIGURE 2. Micro-CT analysis of bone regeneration following treatment of all groups. In first line, it is possible to observe the surface view while in the second line the internal view. In the third line, the region of interest (ROI) was analyzed, from which the data for the Micro-CT was taken.
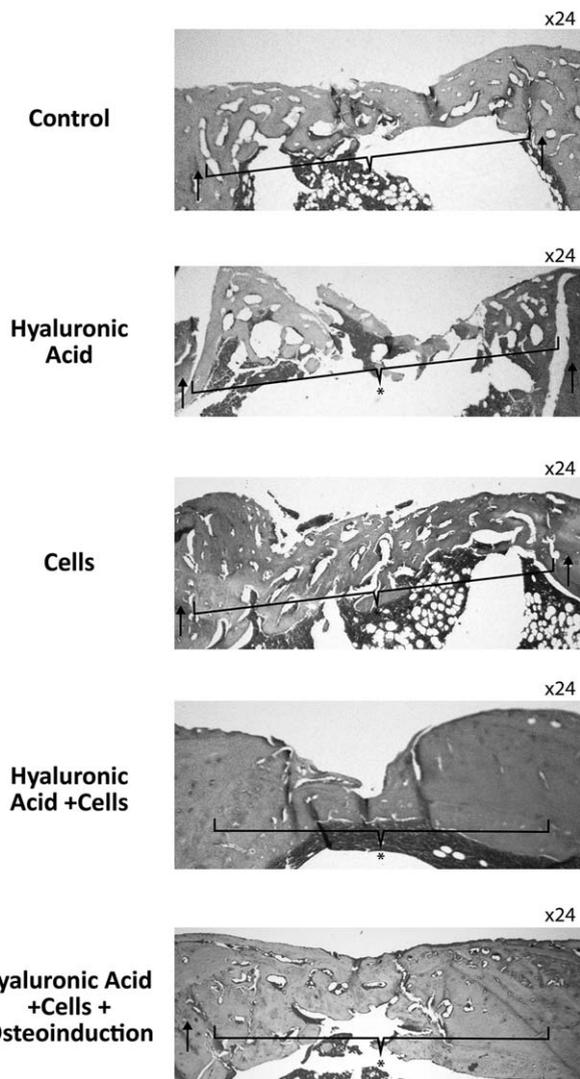

FIGURE 3. Newly regenerated bone in the Control, Hyaluronic Acid, Cells, Hyaluronic Acid + Cells, and Hyaluronic Acid + Cells + Osteoinduction groups was evaluated histologically. Hematoxylin and eosin staining of femur histological sections was performed 23 days after implantation. The arrows indicate the edges of the bone defect and dotted line with asterisks indicated the newly regenerated bone area. The bone bridge images suggested more mature bone formation in the Hyaluronic Acid + Cells and Hyaluronic Acid + Cells + Osteoinduction groups. Inflammatory responses were not observed in any group.

Histological Analysis

Histological analysis is available in Figure 3.

Quantification of Protein Expression by Cells of the Osteogenic Lineage

The SPARC gene expression, which encodes the osteonectin protein, along with the SSP1 gene, which encodes the osteopontin protein, and the COL 1A gene, which encodes type 1 collagen, all of which are expressed during osteogenesis, were evaluated quantitatively using RT-PCR. Expression of the endogenous glyceraldehyde phosphate dehydrogenase (GAPDH) gene was also measured, and its levels were used for normalization of the results.

No significant differences in the expression of collagen type I (Col I) orosteopontin (OP) were observed in any of the experimental groups (Fig. 4A, B). However, the mADSCs group (mean: 2.92) showed a significantly lower level of expression of osteonectin (ON) than the HA (mean: 25.96) and mADSCs osteoin + HA (mean: 25.66) groups (Fig. 4C).
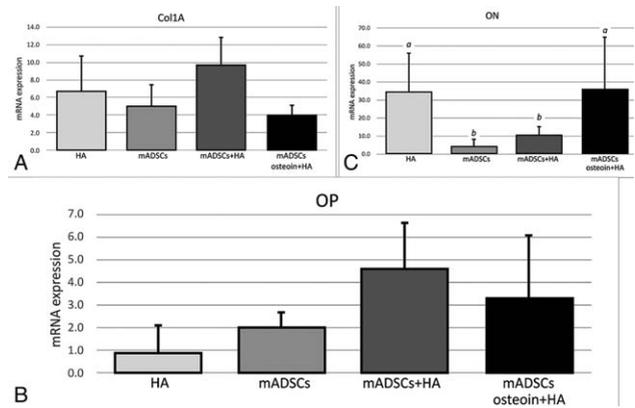

FIGURE 4. (A) Mean and standard deviation of collagen 1A (Col1A) mRNA levels (n = 5 per group). The expression level in the control group was set at 1. (B) Mean and standard deviation of osteopontin (OP) mRNA levels (n = 5 per group). The expression level in the control group was set at 1. (C) Mean and standard deviation of osteonectin (ON) mRNA levels (n = 5 per group). The expression level in the control group was set at 1. The mRNA levels of the HA and mADSCs osteoin + HA groups are significantly different from those of the mADSCs and mADSCs + HA groups ($P < 0.05$).

DISCUSSION

In the present investigation, rat mADSCs were isolated and characterized according to their ability to proliferate as plastic-adherent cells, their phenotypic profile, and their in vitro capacity for differentiation into osteoblasts and adipocytes, fulfilling plainly the criteria of the International Society for Cellular Therapy as true MSCs.[26] Preliminary tests were essential to verify this before proceeding with the in vivo experiments, as bone bioengineering requires MSCs to have plasticity, that is, the ability to overcome lineage barriers and to adopt the phenotypes and gene expression patterns of bone tissue.[27,28]

The selection of donor tissue and chosen cell type plays a very important role in the constitution of the bone tissue engineering triad. With the ability to differentiate into various cell types, including osteogenic lineage cells, mADSCs may be isolated by a less invasive method and offer a much higher yield of MSCs than those obtained by bone marrow aspiration.[29,30] Another major advantage of mADSCs is their ability to release potent growth factors that regulate angiogenesis and extracellular matrix remodeling, such as vascular endothelial growth factor, hepatocyte growth factor, fibroblast growth factor 2, and insulin-like growth factor 1.[31-33]

Histomorphometry, computed microtomography (micro-CT), and RT-PCR were used to quantify and identify the regenerated bone tissue. Three semi-serial sections (300, 600, and 900 μm) were taken from the starting edge of the defect to histologically analyze the region, as established previously.[34] The quantitative results revealed that the cell-containing test groups presented a larger area of newly formed bone compared to control and HA-only groups; in the latter, the histological analysis showed delayed wound healing, along with the presence of bone with tapered trabeculae and red lineage medullary cells. In the groups that received osteoblast-differentiated or nondifferentiated stem cells, there was greater density and bone maturation, being difficult to visually identify the boundaries of the original defect. It was also possible to observe an increase in compact bone tissue and concentric bone deposition presenting Haversian canals.

Several changes in the HA molecule that may improve its function as a scaffold for bone bioengineering have been suggested.[35,36] The physical presentation of HA in the form of HYAFF fibers, when in contact with liquid medium, creates a hydrogel that allows cell incorporation. The hydrogel formulation predominantly used in tissue engineering[35] and also in the present investigation has proven to be applicable both in vitro and in vivo, and has shown promising results when combined with mADSCs, that is, when biomolecules and cells are incorporated into its structure, the regeneration of bone, cartilage, heart, and nerve tissue might be facilitated.[19] However, considering the 23-day regeneration interval, the presence of the scaffold, even when associated with grafted cells, might have acted as a physical barrier also blocking cell migration to the defect. This might have occurred due to the probable incomplete action of the hyaluronidase enzyme, resulting in poorer osteoinductive and osteoconductive responses in the grafted sites, along with the presence of edema, leukocyte aggregation, and postoperative decreased blood flow, leading to the formation of a local organic barrier. Yucel et al[37] confirmed that when applied immediately after the creation of dorsal defects in rats without the presence of adipose stem cells, composite scaffolds undergo necrosis and contraction. However, when the same composites combined with mADSCs were grafted after 4 days, enhanced results were observed. It is important to remember that mADSCs play an important role in angiogenesis, and that their action begin approximately 3 days after grafting,[38,39] concurrent with the release of cytokines such as vascular endothelial growth factor and TGF-β.[38] Furthermore, mADSCs also exercise an immunomodulatory action; their ability to inhibit T cells leads to a decrease in IFN-α production both in vitro and in vivo as well as to increased IL-4 production, thereby changing the immune response profile from pro-inflammatory to anti-inflammatory.[13] However, despite the delayed action of the scaffold used, it was possible to observe the existence of a synergistic effect on bone formation when the applied HA was combined with mADSCs.

The HA hydrogel alone was not able to promote the regeneration of bone tissue in vivo. The HA effect when applied alone can be clearly observed in group II; in this group, less bone formation was detected. This finding may be due to the absence of complete resorption of the HA scaffold, which was not fully replaced by original tissue. While studying tissue regeneration in the craniofacial region, Akizuki et al[40] proposed that periodontal bone defects treated with HA alone should be compared with defects treated with HA combined with periodontal ligament cells. Results for HA alone presented in this investigation are very similar to the results obtained here, in which we observed poorer bone formation than in the HA + cells groups. The presence of the scaffold or even of the biomaterial alone might slow regeneration and reduce its quality.[41,42] Another important issue is the HA degradation process, which affects the biological functions of the compound. Acid degradation products (4−20 disaccharides) have been said to present angiogenic properties and therefore stimulate capillary growth, endothelial proliferation, and blood vessel formation.[43] Results presented here corroborate this assumption through histological sections.

Grafts of MSCs that were previously osteoinduced in vitro and combined with HA were also analyzed. In this regard, the in vitro osteoinduction method, or osteogenic differentiation, requires the presence of β-glycerophosphate, ascorbic acid, and dexamethasone, so that the MSCs can acquire osteoblastic phenotype, beginning to express alkaline phosphatase and deposit a calcium-rich extracellular matrix that includes noncollagenous proteins such as osteopontin and osteonectin.[44,45] This initial stimulus for cell recruitment to the defect site showed no significant difference with respect to the quantity of newly formed tissue compared to the group that received undifferentiated mADSCs. A lack of need for prior osteoinduction in vitro was also demonstrated by Carvalho et al[46] and later by Asutay et al[47] using dental pulp stem cells, as well as by Choi et al[48] when grafting mADSCs and rigid hydroxyapatite scaffolds into bone defects in rats. Results obtained here suggest that by foregoing osteogenic induction it is possible to save time and increase biologic safety as cell in vitro manipulation is reduced. In other in vitro studies in which osteoblastic cells and high-molecular-weight HA (>1000 kDa) were used, inhibition of cell proliferation was demonstrated, whereas low-molecular-weight HA (<50 kDa) stimulated cell proliferation.[49,50]

The micro-CT data obtained 23 days after grafting showed bone tissue interconnection, which is an important condition as the contact between granules provides bridges for the input of osteoblastic cells, blood vessels, and hard tissue growth.[51] Thus, with respect to the bone contact surface, the surface area of mineralized tissue that is interconnected, the mADSCs + HA and mADSCs osteoin + HA groups performed significantly better than the negative control and HA-only groups. A similar result was obtained for bone surface density, the ratio of the total surface area of mineralized tissue to the total volume examined, which quantitatively standardizes all samples. Yang et al[52] also used micro-CT to demonstrate that the use of MSCs combined with a scaffold in critical bone defects led to higher bone density than the use of scaffolds without cells. The micro-CT findings therefore corroborate the histological findings. The significant advantage offered by micro-CT testing is the ability to assess contact surface and surface density of the analyzed region in a precise and nondestructive manner.

It should be noted that a limitation of micro-CT analysis is its thresholding and grayscale image segmentation, which sometimes make it difficult to accurately distinguish the scaffold or remaining biomaterial from newly formed bone.[53] In the present investigation, we did not utilize biomaterials that could be mistaken for bone tissue, making possible to accurately evaluate the effect of HA combined with mADSCs. Moreover, linear attenuation rates were employed to distinguish bone tissue from soft tissue.

The expression of some genes related to osteogenic differentiation was evaluated 23 days after tissue repair with the proposed treatments. RT-PCR revealed that expression of the collagen 1 α-1 gene, which is expressed in mature osteoblasts at a late stage of differentiation,[54] was relatively homogeneous. However, greater expression of this gene was observed in the group treated with undifferentiated mADSCs + HA. The same pattern of gene expression was observed regarding the osteopontin gene. Although there was less expression of OP in the groups treated with HA alone or mADSCs alone, the data indicate an additive effect in the mADSCs + HA group. OP is abundantly secreted by MSCs and can be regulated during their differentiation to the osteogenic stage by its binding to surface markers such as CD44.[55,56] Similarly, as an extracellular matrix component, HA binds to CD44.[57] These characteristics show that CD44, HA, and OP contribute to the expression of specific receptors that facilitate transport, adherence, and infiltration of MSCs to the

injury site.[58,59] According to Beck et al, there is a temporal pattern of typical marker expression according to the osteoblast differentiation phase: proliferation; extracellular matrix deposition and maturation; and mineralization. Alkaline phosphatase, α-1 collagen, and osteonectin show higher expression at the end of the proliferative phase, during the period of extracellular matrix deposition and maturation. The genes expressed in the mineralization phase include osteopontin and osteocalcin.[45] Thus, we can assume consistency in our findings, since we relate the quantity of mineralized bone tissue evidenced by micro-CT and osteonectin expression in the group treated only with undifferentiated mADSCs to that in the mADSCs + HA group, as the respective expression is inversely proportional to the amount of mineralized tissue considering the differentiation stage of the osteoblasts.

CONCLUSION

The results presented here suggest that a combination of HA and mADSCs may offer a promising alternative for bone tissue augmentation. The use of undifferentiated mADSCs facilitates the grafting technique because these cells require less manipulation, which consequently may save time and lower potential biologic risks involved in the process. The molecular weight and physical condition of the applied HA seems to play an important role in the final outcome, indicating that the presence of a scaffold alone without the addition of cells might fail to promote bone regeneration.

Another finding might be the replacement of donor tissue by cells, avoiding the injury on the donor site, thus optimizing conventional grafting treatments. Due to the good results found in our study, as well as the already existent published literature on animal studies, we suggest further studies on human trials for the application in the clinical setting.

REFERENCES

1. Lee SH, Shin H. Matrices and scaffolds for delivery of bioactive molecules in bone and cartilage tissue engineering. *Adv Drug Deliv Rev* 2007;59:339–359
2. Slotte C, Lundgren D, Burgos PM. Placement of autogeneic bone chips or bovine bone mineral in guided bone augmentation: a rabbit skull study. *Int J Oral Maxillofac Implant* 2003;18:795–806
3. Yamada Y, Ueda M, Naiki T, et al. Tissue-engineered injectable bone regeneration for osseointegrated dental implants. *Clin Oral Implant Res* 2004;15:589–597
4. Hibi H, Yamada Y, Kagami H, et al. Distraction osteogenesis assisted by tissue engineering in an irradiated mandible: a case report. *Int J Oral Maxillofac Implant* 2006;21:141–147
5. Ueda M, Yamada Y, Ozawa R, et al. Clinical case reports of injectable tissue-engineered bone for alveolar augmentation with simultaneous implant placement. *Int J Periodontics Restor Dent* 2005;25:129–137
6. Ohya M, Yamada Y, Ozawa R, et al. Sinus floor elevation applied tissue-engineered bone. Comparative study between mesenchymal stem cells/platelet-rich plasma (PRP) and autogenous bone with PRP complexes in rabbits. *Clin Oral Implant Res* 2005;16:622–629
7. Ito K, Yamada Y, Nagasaka T, et al. Osteogenic potential of injectable tissue-engineered bone: a comparison among autogenous bone, bone substitute (Bio-oss), platelet-rich plasma, and tissue-engineered bone with respect to their mechanical properties and histological findings. *J Biomed Mater Res A* 2005;73:63–72
8. Ueda M, Yamada Y, Kagami H, et al. Injectable bone applied for ridge augmentation and dental implant placement: human progress study. *Implant Dent* 2008;17:82–90
9. Boeckel DG, Shinkai RS, Grossi ML, et al. Cell culture-based tissue engineering as an alternative to bone grafts in implant dentistry: a literature review. *J Oral Implant* 2012;38 (Spec No):538–545
10. Kaigler D, Mooney D. Tissue engineering's impact on dentistry. *J Dent Educ* 2001;65:456–462
11. Jiang Y, Jahagirdar BN, Reinhardt RL, et al. Pluripotency of mesenchymal stem cells derived from adult marrow. *Nature* 2002;418:41–49
12. Colter DC, Class R, DiGirolamo CM, et al. Rapid expansion of recycling stem cells in cultures of plastic-adherent cells from human bone marrow. *Proc Natl Acad Sci U S A* 2000;97:3213–3218
13. Osugi M, Katagiri W, Yoshimi R, et al. Conditioned media from mesenchymal stem cells enhanced bone regeneration in rat calvarial bone defects. *Tissue Eng Part A* 2012;18:1479–1489
14. Gnecchi M, Zhang Z, Ni A, et al. Paracrine mechanisms in adult stem cell signaling and therapy. *Circ Res* 2008;103:1204–1219
15. Ratajczak MZ, Jadczyk T, Pedziwiatr D, et al. New advances in stem cell research: practical implications for regenerative medicine. *Pol Arch Med Wewn* 2014;124:417–426
16. Inukai T, Katagiri W, Yoshimi R, et al. Novel application of stem cell-derived factors for periodontal regeneration. *Biochem Biophys Res Commun* 2013;430:763–768
17. Kaigler D, Cirelli JA, Giannobile WV. Growth factor delivery for oral and periodontal tissue engineering. *Expert Opin Drug Deliv* 2006;3:647–662
18. Nauta AJ, Westerhuis G, Kruisselbrink AB, et al. Donor-derived mesenchymal stem cells are immunogenic in an allogeneic host and stimulate donor graft rejection in a nonmyeloablative setting. *Blood* 2006;108:2114–2120
19. Kim J, Kim IS, Cho TH, et al. Bone regeneration using hyaluronic acid-based hydrogel with bone morphogenic protein-2 and human mesenchymal stem cells. *Biomaterials* 2007;28:1830–1837
20. Poldervaart MT, Goversen B, de Ruijter M, et al. 3D bioprinting of methacrylated hyaluronic acid (MeHA) hydrogel with intrinsic osteogenicity. *PLoS One* 2017;12:e0177628
21. Stern M, Longaker MT, Adzick S, et al. Wound healing and regeneration in a fetalcleft lip model. In: Lynch SE, Genco RJ, Marx RE, eds. *Tissue Engineering Applications in Maxillofacial Surgery and Periodontics.* Chicago, IL: Quintessence; 1999:55–68
22. Prè ED, Conti G, Sbarbati A. Hyaluronic acid (HA) scaffolds and multipotent stromal cells (MSCs) in regenerative medicine. *Stem Cell Rev* 2016;12:664–681
23. Meirelles LdaS, Nardi NB. Murine marrow-derived mesenchymal stem cell: isolation, in vitro expansion, and characterization. *Br J Haematol* 2003;123:702–711
24. Gibson UE, Heid CA, Williams PM. A novel method for real time quantitative RT-PCR. *Genome Res* 1996;6:995–1001
25. Heid CA, Stevens J, Livak KJ, et al. Real time quantitative PCR. *Genome Res* 1996;6:986–994
26. Dominici M, Le Blanc K, Mueller I, et al. Minimal criteria for defining multipotent mesenchymal stromal cells. The International Society for Cellular Therapy position statement. *Cytotherapy* 2006;8:315–317
27. Horst OV, Chavez MG, Jheon AH, et al. Stem cell and biomaterials research in dental tissue engineering and regeneration. *Dent Clin North Am* 2012;56:495–520
28. Neel EA, Chrzanowski W, Salih VM, et al. Tissue engineering in dentistry. *J Dent* 2014;42:915–928
29. Mizuno H. Adipose-derived stem cells for tissue repair and regeneration: ten years of research and a literature review. *J Nippon Med Sch* 2009;76:56–66
30. Gimble JM, Katz AJ, Bunnell BA. Adipose-derived stem cells for regenerative medicine. *Circ Res* 2007;100:1249–1260
31. Rehman J, Traktuev D, Li J, et al. Secretion of angiogenic and antiapoptotic factors by human adipose stromal cells. *Circulation* 2004;109:1292–1298
32. Cao Y, Sun Z, Liao L, et al. Human adipose tissue-derived stem cells differentiate into endothelial cells in vitro and improve postnatal neovascularization in vivo. *Biochem Biophys Res Commun* 2005;332:370–379
33. Nakagami H, Maeda K, Morishita R, et al. Novel autologous cell therapy in ischemic limb disease through growth factor secretion by cultured adipose tissue-derived stromal cells. *Arter Thromb Vasc Biol* 2005;25:2542–2547
34. de Mello ED, Pagnoncelli RM, Munin E, et al. Comparative histological analysis of bone healing of standardized bone defects performed with the Er:YAG laser and steel burs. *Lasers Med Sci* 2008;23:253–260

35. Prestwich GD, Marecak DM, Marecek JF, et al. Controlled chemical modification of hyaluronic acid: synthesis, applications, and biodegradation of hydrazide derivatives. *J Control Release* 1998;53:93–103

36. Monzack EL, Rodriguez KJ, McCoy CM, et al. Natural materials in tissue engineering applications. In: Burdick J, Mauck ARL, eds. *Biomaterials for Tissue Engineering Applications: A Review of the Past and Future Trends.* Berlin: Springer-Verlag/Wien; 2011:209–241

37. Yucel E, Alagoz MS, Eren GG, et al. Use of adipose-derived mesenchymal stem cells to increase viability of composite grafts. *J Craniofac Surg* 2016;27:1354–1360

38. Nie C, Yang D, Xu J, et al. Locally administered adipose-derived stem cells accelerate wound healing through differentiation and vasculogenesis. *Cell Transpl* 2011;20:205–216

39. Zografou A, Papadopoulos O, Tsigris C, et al. Autologous transplantation of adipose-derived stem cells enhances skin graft survival and wound healing in diabetic rats. *Ann Plast Surg* 2013;71:225–232

40. Akizuki T, Oda S, Komaki M, et al. Application of periodontal ligament cell sheet for periodontal regeneration: a pilot study in beagle dogs. *J Periodontal Res* 2005;40:245–251

41. Lindhe J, Cecchinato D, Donati M, et al. Ridge preservation with the use of deproteinized bovine bone mineral. *Clin Oral Implant Res* 2014;25:786–790

42. Bartold PM, McCulloch CA, Narayanan AS, et al. Tissue engineering: a new paradigm for periodontal regeneration based on molecular and cell biology. *Periodontol 2000* 2000;24:253–269

43. Allison DD, Grande-Allen KJ. Review. Hyaluronan: a powerful tissue engineering tool. *Tissue Eng* 2006;12:2131–2140

44. Im GI, Shin YW, Lee KB. Do adipose tissue-derived mesenchymal stem cells have the same osteogenic and chondrogenic potential as bone marrow-derived cells? *Osteoarthr Cartil* 2005;13:845–853

45. Beck GR Jr, Zerler B, Moran E. Phosphate is a specific signal for induction of osteopontin gene expression. *Proc Natl Acad Sci U S A* 2000;97:8352–8357

46. Carvalho PP, Leonor IB, Smith BJ, et al. Undifferentiated human adipose-derived stromal/stem cells loaded onto wet-spun starch-polycaprolactone scaffolds enhance bone regeneration: nude mice calvarial defect in vivo study. *J Biomed Mater Res A* 2014;102:3102–3111

47. Asutay F, Polat S, Gul M, et al. The effects of dental pulp stem cells on bone regeneration in rat calvarial defect model: micro-computed tomography and histomorphometric analysis. *Arch Oral Biol* 2015;60:1729–1735

48. Choi JW, Park EJ, Shin HS, et al. In vivo differentiation of undifferentiated human adipose tissue-derived mesenchymal stem cells in critical-sized calvarial bone defects. *Ann Plast Surg* 2014;72:225–233

49. Pilloni A, Bernard GW. The effect of hyaluronan on mouse intramembranous osteogenesis in vitro. *Cell Tissue Res* 1998;294:323–333

50. Kunze R, Rosler M, Moller S, et al. Sulfated hyaluronan derivatives reduce the proliferation rate of primary rat calvarial osteoblasts. *Glycoconj J* 2010;27:151–158

51. Lutolf MP, Weber FE, Schmoekel HG, et al. Repair of bone defects using synthetic mimetics of collagenous extracellular matrices. *Nat Biotechnol* 2003;21:513–518

52. Yang Y, Hallgrimsson B, Putnins EE. Craniofacial defect regeneration using engineered bone marrow mesenchymal stromal cells. *J Biomed Mater Res A* 2011;99:74–85

53. Polak SJ, Candido S, Levengood SK, et al. Automated segmentation of micro-CT images of bone formation in calcium phosphate scaffolds. *Comput Med Imaging Graph* 2012;36:54–65

54. Rickard DJ, Sullivan TA, Shenker BJ, et al. Induction of rapid osteoblast differentiation in rat bone marrow stromal cell cultures by dexamethasone and BMP-2. *Dev Biol* 1994;161:218–228

55. Wang KX, Denhardt DT. Osteopontin: role in immune regulation and stress responses. *Cytokine Growth Factor Rev* 2008;19:333–345

56. Chen Q, Shou P, Zhang L, et al. An osteopontin-integrin interaction plays a critical role in directing adipogenesis and osteogenesis by mesenchymal stem cells. *Stem Cells* 2014;32:327–337

57. Gerdin B, Hallgren R. Dynamic role of hyaluronan (HYA) in connective tissue activation and inflammation. *J Intern Med* 1997;242:49–55

58. Sano N, Kitazawa K, Sugisaki T. Localization and roles of CD44, hyaluronic acid and osteopontin in IgA nephropathy. *Nephron* 2001;89:416–421

59. Barbash IM, Chouraqui P, Baron J, et al. Systemic delivery of bone marrow-derived mesenchymal stem cells to the infarcted myocardium: feasibility, cell migration, and body distribution. *Circulation* 2003;108:863–868